Combined thioflavin T–Congo red fluorescence assay for amyloid fibril detection

Methods and Applications in Fluorescence

PAPER

Combined thioflavin T–Congo red fluorescence assay for amyloid fibril detection

Mykhailo Girych[1,3,4,5], Galyna Gorbenko[1], Ivan Maliyov[1], Valeriya Trusova[1], Chiharu Mizuguchi[2], Hiroyuki Saito[2] and Paavo Kinnunen[3]

1   Department of Nuclear and Medical Physics, V.N. Karazin Kharkiv National University, 4 Svobody Sq., Kharkiv 61022, Ukraine
2   Department of Biophysical Chemistry, Kyoto Pharmaceutical University, 5 Nakauchi-cho, Misasagi, Yamashina-ku, Kyoto 607-8414, Japan
3   Department of Neuroscience and Biomedical Engineering, School of Science and Technology, Aalto University, FI-00076, Espoo, Finland
4   Author to whom any correspondence should be addressed
5   19/2 Tankopiya Str., ap. 47, Kharkov 61091, Ukraine

E-mail: girychms@gmail.com

Abstract

Fluorescence represents one of the most powerful tools for the detection and structural characterization of the pathogenic protein aggregates, amyloid fibrils. The traditional approaches to the identification and quantification of amyloid fibrils are based on monitoring the fluorescence changes of the benzothiazole dye thioflavin T (ThT) and absorbance changes of the azo dye Congo red (CR). In routine screening it is usually sufficient to perform only the ThT and CR assays, but both of them, when used separately, could give false results. Moreover, fibrillization kinetics can be measured only by ThT fluorescence, while the characteristic absorption spectra and birefringence of CR represent more rigid criteria for the presence of amyloid fibrils. Therefore, it seemed reasonable to use both these dyes simultaneously, combining the advantages of each technique. To this end, we undertook a detailed analysis of the fluorescence spectral behavior of these unique amyloid tracers upon their binding to amyloid fibrils from lysozyme, insulin and an N-terminal fragment of apolipoprotein A-I with Iowa mutation. The fluorescence measurements revealed several criteria for distinguishing between fibrillar and monomeric protein states: (i) a common drastic increase in ThT fluorescence intensity; (ii) a sharp decrease in ThT fluorescence upon addition of CR; (iii) an appearance of the maximum at 535–540 nm in the CR excitation spectra; (iv) increase in CR fluorescence intensity at 610 nm. Based on these findings we designed a novel combined ThT–CR fluorescence assay for amyloid identification. Such an approach not only strengthens the reliability of the ThT assay, but also provides new opportunities for structural characterization of amyloid fibrils.

1. Introduction

Among the huge variety of fluorescence applications in biology and medicine one of the most important is the use of fluorescence-based assays for the identification and structural analysis of a particular type of protein aggregates, amyloid fibrils. These aggregates are currently the focus of tremendous research effort because of their involvement in the pathogenesis of numerous disorders including neurological diseases, type II diabetes, systemic amyloidosis, etc [1, 2]. A distinctive feature of amyloid assemblies is a core

β-sheet structure with the solvent-exposed grooves being spanned across consecutive β-strands parallel to the fibril axis [3]. The presence of such grooves is thought to be critical in determining the ability of amyloid-specific chromo- and fluorophores to associate with fibrillar assemblies, and undergo a characteristic change in their spectral properties [4]. One of the most widespread criteria for the identification and quantification of amyloid fibrils consists in exploring the fluorescence responses of the benzothiazole dye thioflavin T (ThT) [5]. The binding of ThT to fibrillar aggregates is accompanied by considerable
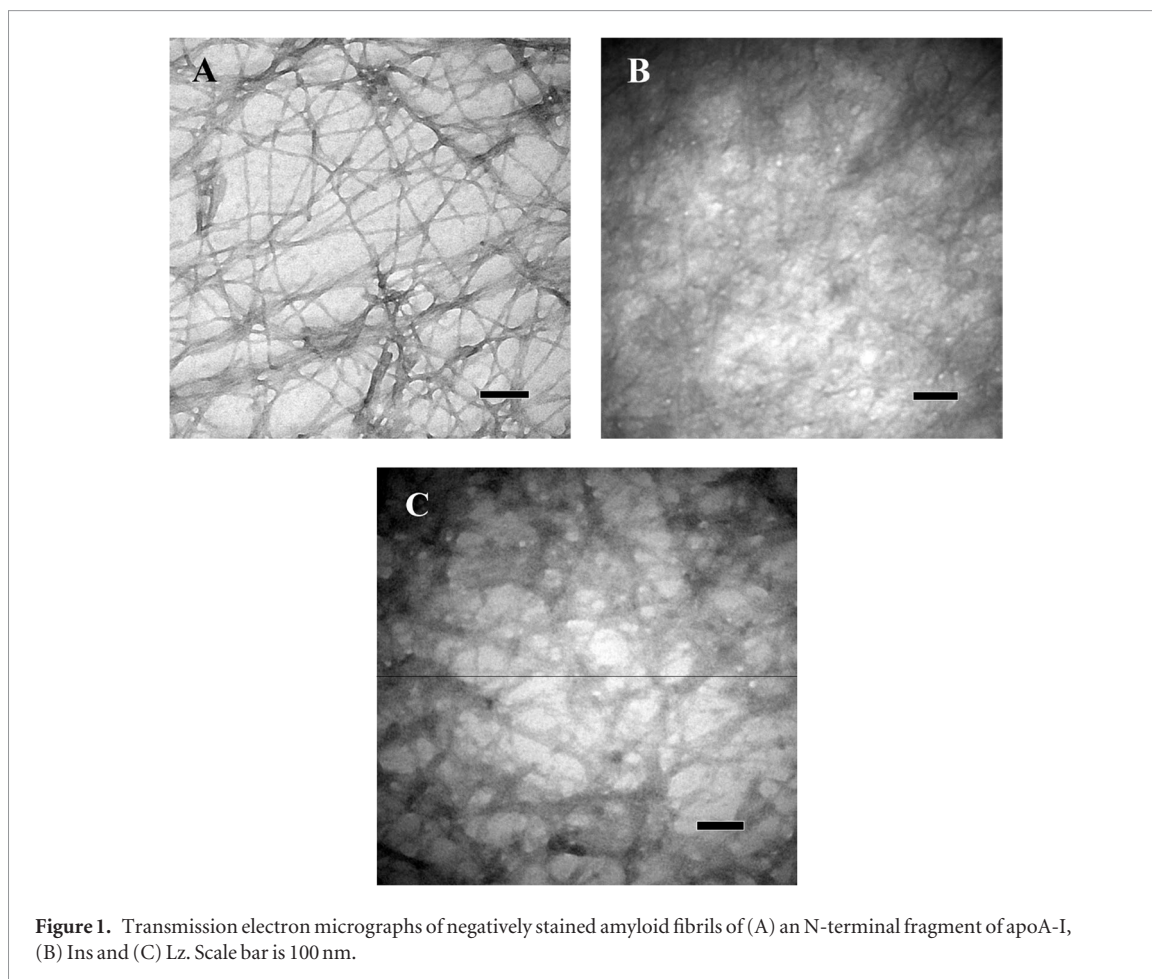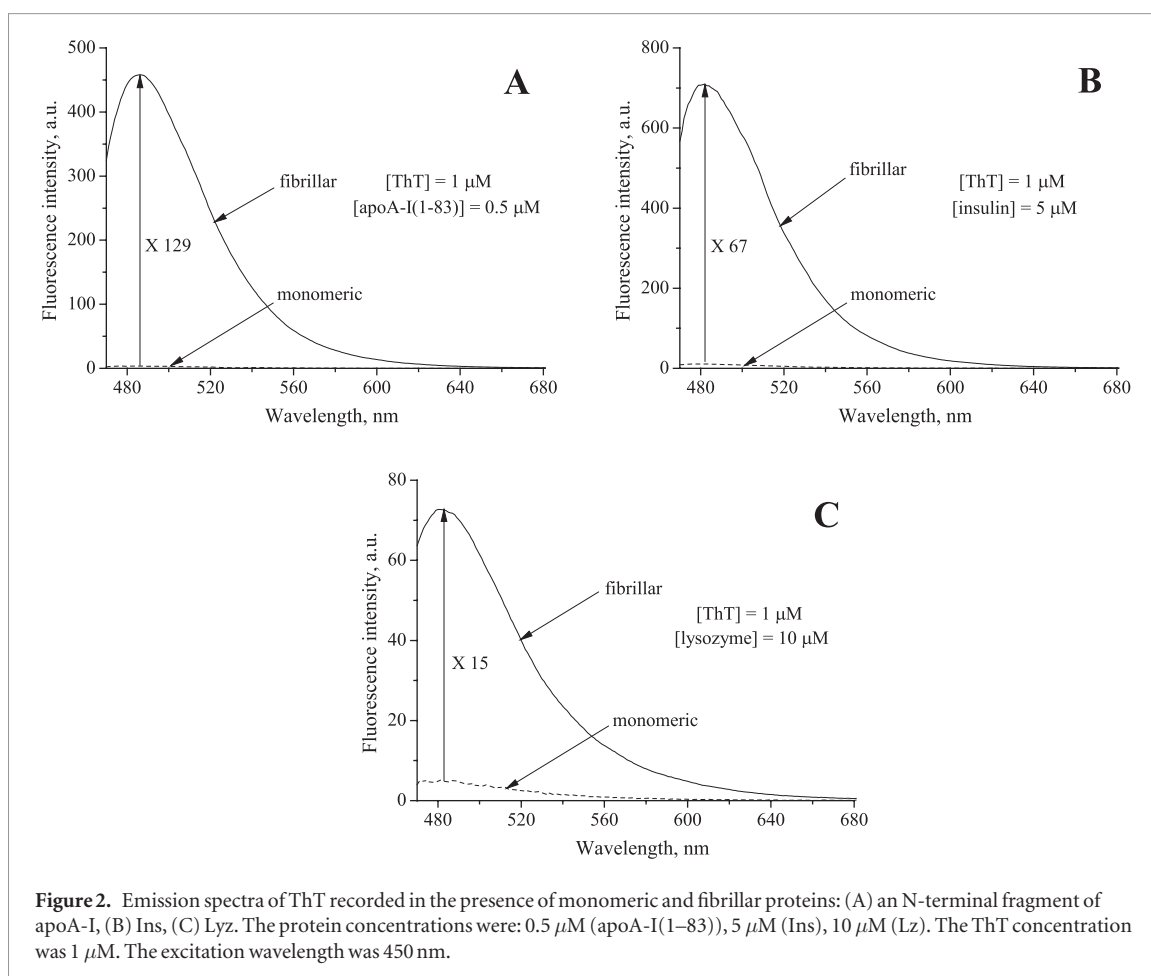
Figure 1. Transmission electron micrographs of negatively stained amyloid fibrils of (A) an N-terminal fragment of apoA-I, (B) Ins and (C) Lz. Scale bar is 100 nm.

long-wavelength shifts of its excitation and emission bands, coupled with a dramatic fluorescence upsurge that can be of several orders of magnitude depending on the fibril type [4, 6]. This effect is interpreted as arising from a significant restriction of the torsional oscillations of the benzothiazole and aminobenzoyl rings of the dye lodging within the fibril groove [7–9]. This mode of the dye–protein complexation prevents the formation of a weakly fluorescent twisted internal charge-transfer state and renders the ThT molecule nearly planar [8]. Although ThT assay is considered to be a golden standard for amyloid fibril detection, a number of studies report that in some cases it can give false positive results. For example, amyloid-specific fluorescence enhancement of ThT is observed in the presence of native γ-CD [10] and AChE [11], oligomeric β-lactoglobulin [12], SDS micells [13], and DNA [14].

Another dye that has traditionally been used as amyloid marker is Congo red (CR), a symmetrical azo dye containing both nonpolar and polar moieties. The nonpolar moiety of CR is composed of the central biphenyl group linked through diazo bonds to two flanked naphthalene rings, while the polar part is represented by the amino groups and negatively charged sulfate groups linked to the naphthalene rings. The association of CR with amyloid assemblies produces a characteristic green–yellow birefringence under polarized light and a shift of the absorption maximum from

~490 nm to ~540 nm [15]. To explain the mechanisms of CR-fibril binding, two hypotheses have been proposed [16–22]. Of these, the first suggests that ionic and hydrophobic dye–protein interactions favor the alignment of the CR molecule within the grooves along the fibril axis [15, 19–21], while the second postulates that CR molecules orient perpendicular to the fibril direction, intercalating between two β-strands in the antiparallel β-sheets [17, 18]. As for the amyloid specificity of CR, false positive results have been reported only in case of birefringence assay [23], whereas a CR spectroscopic test is regarded as a more objective and reliable way of detecting amyloid fibrils [24].

Being inspired by the remarkable properties of ThT and CR, we came to the idea that the amyloid-sensing abilities of these dyes can be exploited in the same fluorescence-based amyloid assay with higher informativity, improved sensitivity and improved reliability compared to the traditional ThT test. To verify the validity of this idea, in the present study we examined the fibrillar aggregates of three proteins, lysozyme (Lz), insulin (Ins) and an N-terminal fragment of apolipoprotein A-I (apoA-I), using a fluorescence assay involving both amyloid-specific dyes, ThT and CR. Our main goal was to evaluate the possibility of designing the combined ThT–CR amyloid test through identifying the spectral parameters that can serve as the signs of amyloid formation complementary to the commonly measured ThT fluorescence increase.

Figure 2. Emission spectra of ThT recorded in the presence of monomeric and fibrillar proteins: (A) an N-terminal fragment of apoA-I, (B) Ins, (C) Lyz. The protein concentrations were: 0.5 μM (apoA-I(1–83)), 5 μM (Ins), 10 μM (Lz). The ThT concentration was 1 μM. The excitation wavelength was 450 nm.

2. Materials and methods

2.1. Chemicals

Chicken egg white Lz, bovine Ins, ThT, and CR, Tris, sodium chloride, sodium azide, and hydrochloric acid were purchased from Sigma (USA). The N-terminal 1–83 fragment of human apoA-I(1–83) with Iowa mutation (G26R) was expressed and purified as described elsewhere [25]. The apoA-I preparations were at least 95% pure as assessed by SDS-PAGE. The dye and protein concentrations were determined spectrophotometrically.

2.2. Fibril preparation

The Ins and Lz fibrils were formed by the incubation of the protein solutions (1 mM) in deionized water (pH 2.0) at 60 °C over 14–20 d [26, 27]. An N-terminal 1–83 fragment of apoA-I was freshly dialyzed from 6 M guanidine hydrochloride solution into 10 mM Tris buffer, 150 mM NaCl, 0.01% NaN$_3$, pH 7.4 before use. The reaction of protein fibrillization was conducted at 37 °C in the above buffer (50 μM of protein) with constant agitation on an orbital shaker [25]. The amyloid nature of the fibrillar aggregates was confirmed by transmission electron microscopy and ThT assay.

2.3. Transmission electron microscopy

For the electron microscopy assay, a 10 μl drop of the protein solution (taken from the tested sample after

finishing the fibril growth) was applied to a carbon-coated grid and blotted after 1 min. A 10 μl drop of 2% (w/v) uranyl acetate solution was placed on the grid, blotted after 30 s, and then washed five times in deionized water and air dried. The resulting grids were viewed by a Jeol JSM-840 or Tecnai 12 BioTWIN electron microscope.

2.4. Steady-state fluorescence measurements

Steady-state fluorescence spectra of the dyes were recorded with a Varian Cary Eclipse (Varian Instruments, Walnut Creek, CA) spectrofluorimeter equipped with a magnetically stirred, thermostated cuvette holder. Fluorescence measurements were performed at 20 °C using 10 mm path-length quartz cuvettes with 2 ml of sample. The excitation and emission slit widths were set at 10 nm. Emission and excitation spectra were recorded with excitation wavelengths of 450 nm for ThT and emission wavelength of 610 nm for CR. The fluorescence intensity of ThT measured in the presence of CR was corrected for the reabsorption and inner filter effects using the following coefficients [28]:

$$k = \frac{(1 - 10^{-A_{ThT}^{ex}})(A_{ThT}^{ex} + A_{CR}^{ex})(1 - 10^{-A_{ThT}^{em}})(A_{ThT}^{em} + A_{CR}^{em})}{(1 - 10^{-(A_{ThT}^{ex} + A_{CR}^{ex})})A_{ThT}^{ex}(1 - 10^{-(A_{ThT}^{em} + A_{CR}^{em})})A_{ThT}^{em}}$$

(1)

where A_{ThT}^{ex} and A_{ThT}^{em} are the ThT optical densities at the excitation and emission wavelengths in the absence
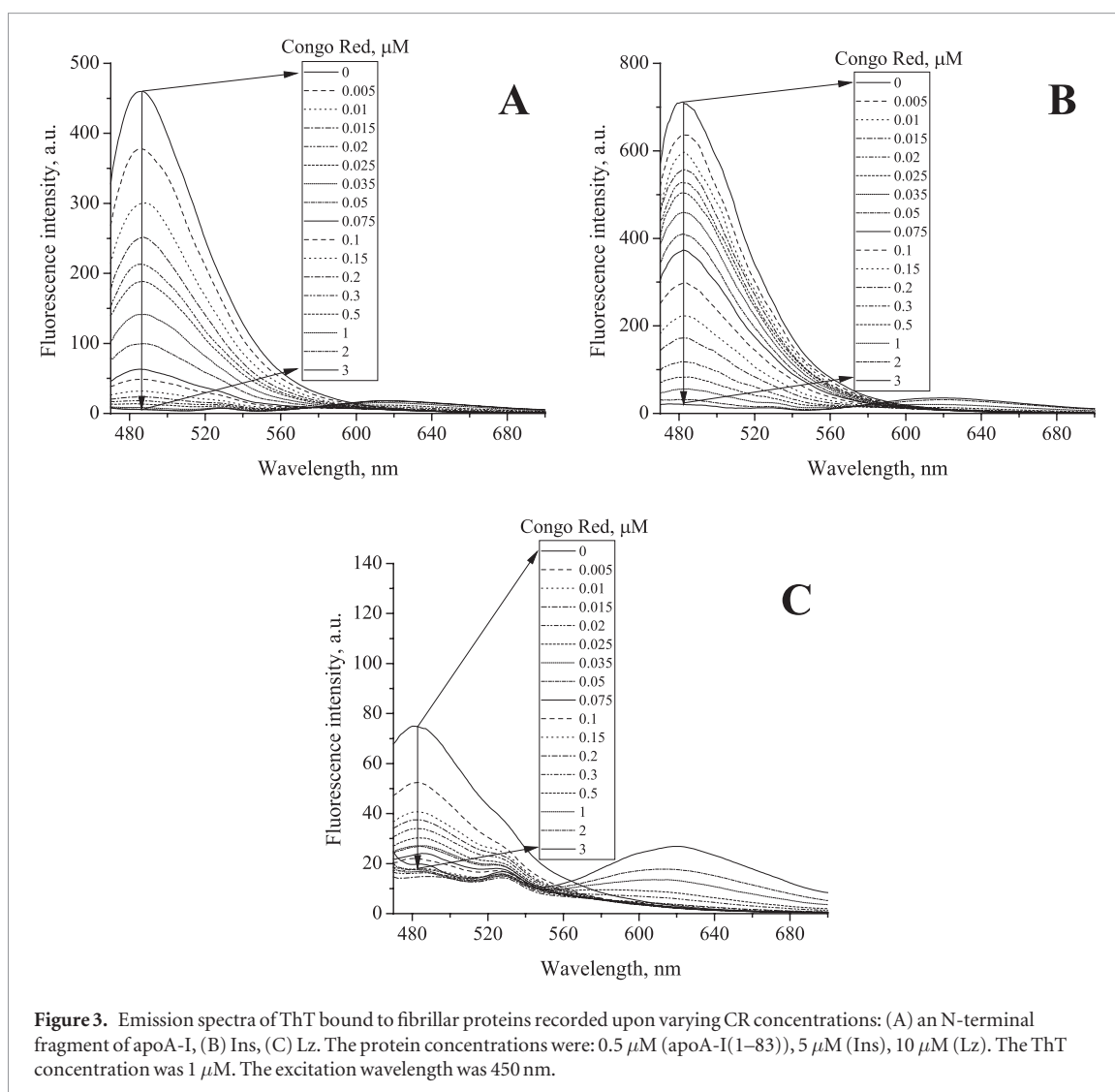
Figure 3. Emission spectra of ThT bound to fibrillar proteins recorded upon varying CR concentrations: (A) an N-terminal fragment of apoA-I, (B) Ins, (C) Lz. The protein concentrations were: 0.5 μM (apoA-I(1–83)), 5 μM (Ins), 10 μM (Lz). The ThT concentration was 1 μM. The excitation wavelength was 450 nm.

of CR, and A_{CR}^{ex} and A_{CR}^{em} are the CR optical densities at the excitation and emission wavelengths, respectively.

The critical distance of energy transfer for the donor–acceptor pair ThT–CR was calculated as [29]:

$$R_o = 979(\kappa^2 n_r^{-4} Q_D J)^{1/6},$$
$$J = \int_0^\infty F_D(\lambda)\varepsilon_A(\lambda)\lambda^4 d\lambda \bigg/ \int_0^\infty F_D(\lambda)d\lambda \quad (2)$$

where J is the overlap integral derived from numerical integration, $F_D(\lambda)$ is the donor fluorescence intensity, $\varepsilon_A(\lambda)$ is the acceptor molar absorbance at the wavelength λ, n_r is the refractive index of the medium ($n_r = 1.4$), Q_D is the donor quantum yield, κ^2 is an orientation factor. Assuming random reorientation of the donor emission and acceptor absorption transition moments during the emission lifetime ($\kappa^2 = 0.67$) the R_o value for the donor–acceptor pair ThT–CR was estimated to be ~4 nm.

3. Results and discussion

3.1. Amyloid-specific changes in the emission spectra of ThT

As illustrated in figure 1, the incubation of the examined proteins under amyloidogenic conditions

gives rise to the formation of clearly visible fibrillar amyloid structures with specific morphologies (see also supplementary figure 1 (stacks.iop.org/ MAF/4/034010/mmedia)). The observed differences in fibril morphology are consistent with the data reported elsewhere and stem presumably from the distinctions in the structure of β-pleated core of amyloid protofilaments [30, 31]. Figure 2 shows that the association of ThT molecules with fibrillar proteins resulted in an expected drastic increase of fluorescence intensity upon excitation at 450 nm, the wavelength at which fibril-bound molecules of the dye are preferably excited. While being extrapolated to the same protein-to-ThT molar ratio 1:0.5, the maximum fluorescence intensities follow the order apoA-I (450) > Ins (~70) > Lz (~4). Such discrepancies, as demonstrated previously, may originate from the differences in the affinity and accessibility of fibrillar binding sites on the β-pleated sheets which, in turn, may be a consequence of the diversity of protofilament structures [4, 32].

As seen in figure 3, the addition of CR to the fibril-ThT mixtures was followed by a sharp decrease in ThT fluorescence intensity and the appearance of a CR emission peak at 620 nm. Notably, a significant decrease in ThT fluorescence is already seen at low
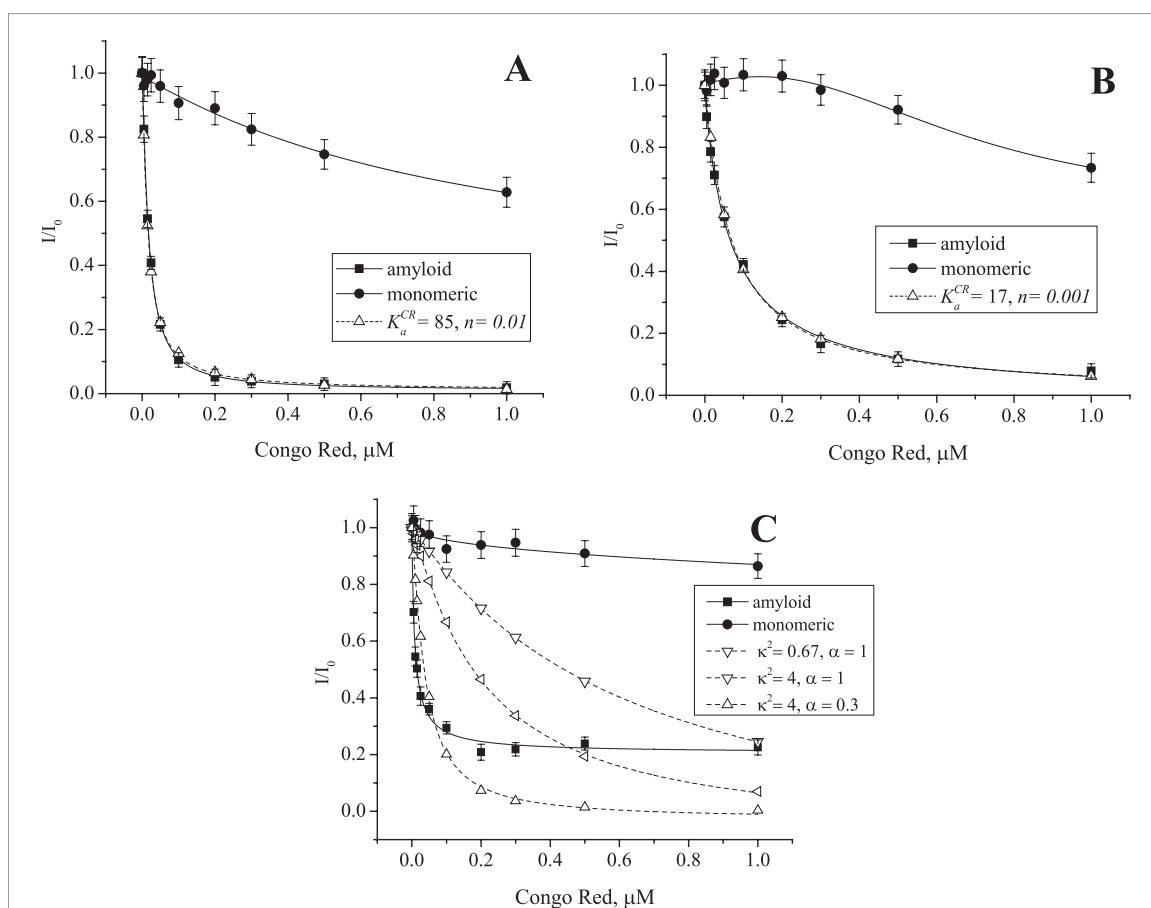
Figure 4. Relative decrease in ThT fluorescence at 484 nm as a function of CR concentration: (A) an N-terminal fragment of apoA-I, (B) Ins, (C) Lz. The ThT concentration was 1 μM. The hollow symbols depict the values of the relative quantum yield calculated in terms of the competition binding model (equation (3)) with the following set of parameters: (A) $K_a^{ThT} = 0.1$, $K_a^{CR} = 85$, $n = 0.01$ and (B) $K_a^{ThT} = 0.1$, $K_a^{CR} = 17$, $n = 0.001$. (C) The hollow symbols depict the values of the relative quantum yield calculated in terms of the stretched exponential model (equation (4)).
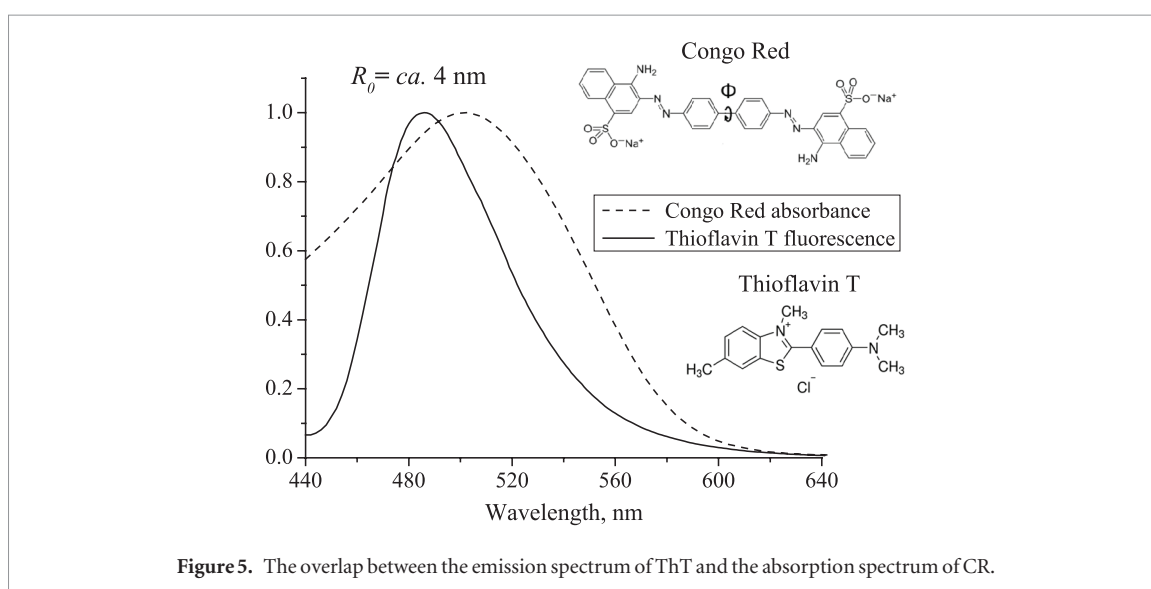
Figure 5. The overlap between the emission spectrum of ThT and the absorption spectrum of CR.

CR concentrations (at ThT-to-CR molar ratio 100:1), whereas the equal molar ratio of the dyes results in the drastic quenching of ThT bound to apoA-I(1–83) and Ins fibrils (figure 4). Likewise, the titration of ThT-fibrillar Lz mixtures with CR revealed that the extent of CR-induced fluorescence quenching does not exceed 80%. This observation can be explained either by the presence of a substantial amount of monomeric/oligo-meric protein species, which are poorly quenched by CR (as described below), or by the reduced accessibility of ThT binding sites within Lz fibrils for CR molecules. Unlike the fibrillar aggregates, in the ThT mixtures with

Figure 6. Excitation spectra of CR recorded upon the addition of dye to the solution of fibrillar (A) apoA-I (1–83), (B) Ins, (C) Lz. The protein concentrations were: 0.5 μM (apoA-I (1–83)), 5 μM (Ins), 10 μM (Lz). The ThT concentration was 1 μM. The emission wavelength was 610 nm.
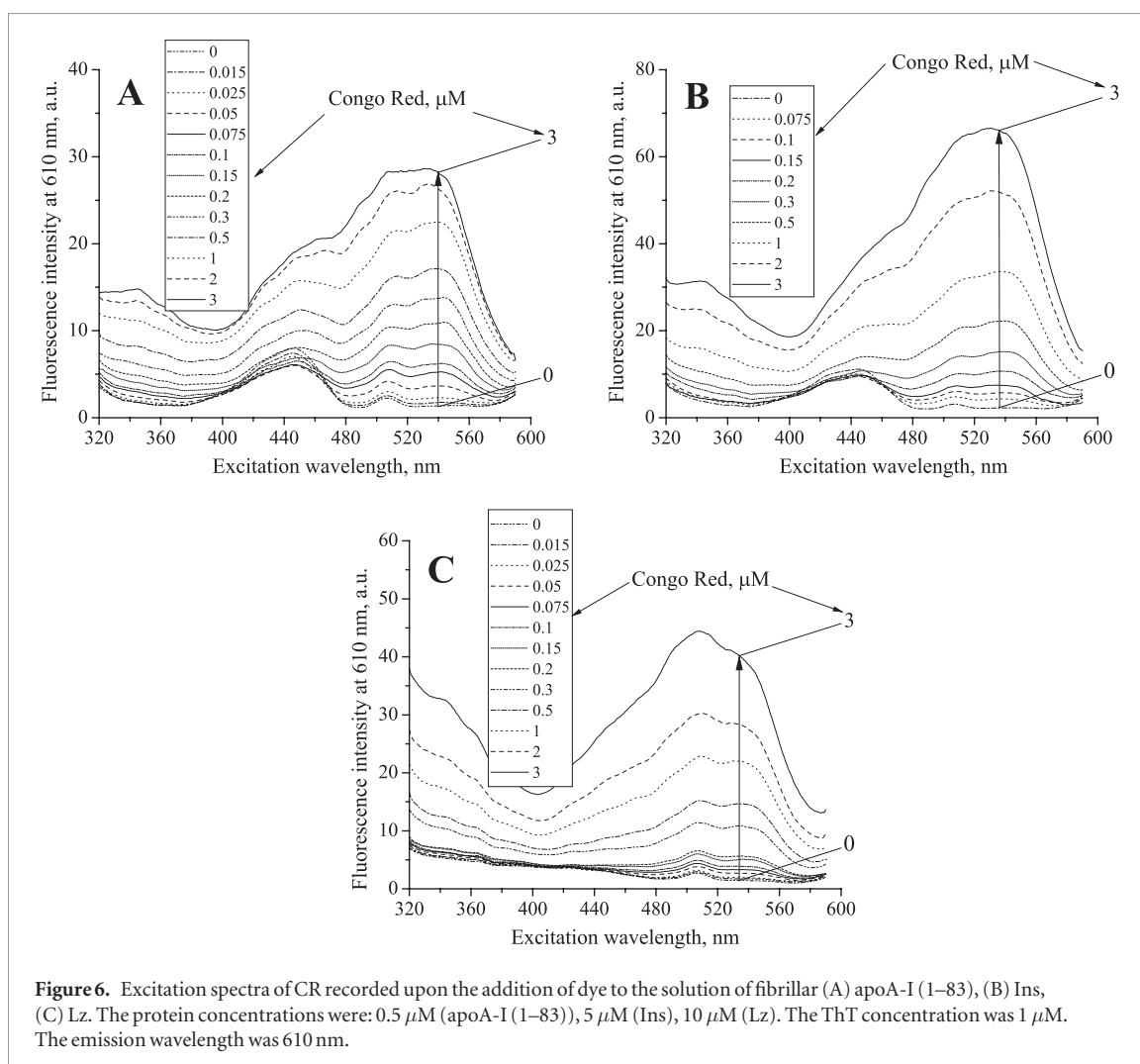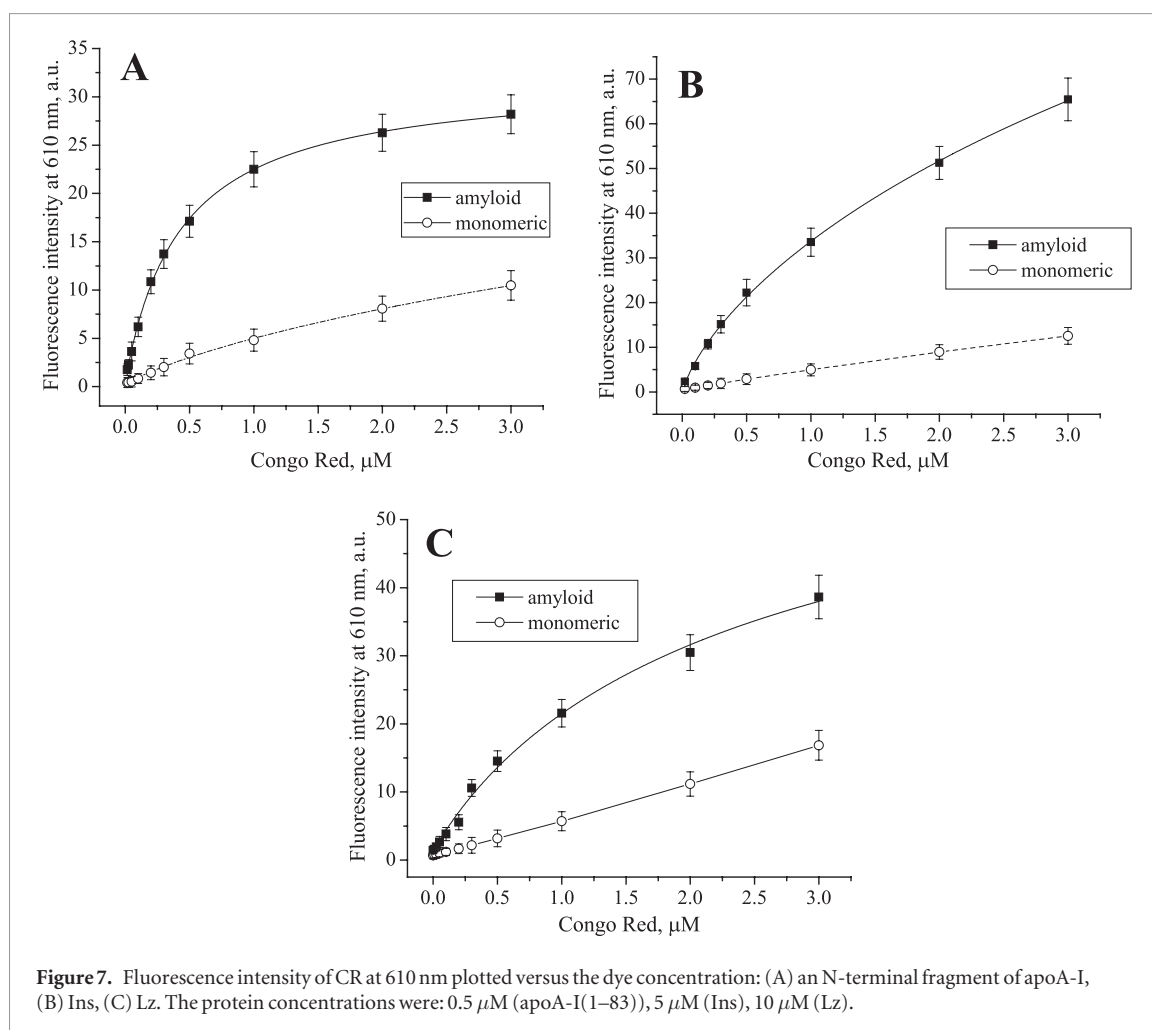
monomeric proteins CR was able to induce noticeable fluorescence quenching only at high concentrations. Furthermore, there was no detectable decrease in ThT fluorescence in the protein-free titrations (data not shown). All the above findings led us to conclude that such a striking decrease in ThT fluorescence in the presence of CR is highly specific to the β-sheet motif of amyloid protofilaments. It is noteworthy that CR has previously been shown to reduce the fluorescence of amyloid-bound ThT at rather high concentrations. In particular, at concentrations more than 1.5 μM, CR was able to quench the fluorescence of ThT on Ab(1–40) and Ab(1–42) fibrils [33–35]. Our findings agree with these observations but also indicate that they occur even at sub-micromolar concentrations of CR with a ThT-to-CR molar ratio 100:1. To rationalize this effect, we analyzed three possible reasons for the quenching of ThT fluorescence by CR: (i) the competition between CR and ThT molecules for the binding sites on amyloid β-sheet surface; (ii) direct complexation between ThT and CR on the fibril template; (iii) Förster resonance energy transfer (FRET) from ThT to CR by the Förster mechanism. In an attempt to test the competition hypothesis, we simulated the process of competitive binding using the traditional Langmuir adsorption model. The concentrations of fibril-bound ThT (B_{ThT})

and CR (B_{CR}) were calculated by the numerical solving of the system of two equations:

$$K_a^{ThT} - \frac{B_{ThT}}{(nP - B_{ThT} - B_{CR})(Z_{ThT} - B_{ThT})} = 0$$

$$K_a^{CR} - \frac{B_{CR}}{(nP - B_{ThT} - B_{CR})(Z_{CR} - B_{CR})} = 0 \qquad (3)$$

where K_a^{ThT}, K_a^{CR} are the association constants, Z_{ThT}, Z_{CR} are the total concentrations of ThT and CR, respectively, n is the binding stoichiometry, and P is the total protein concentration. Given that the intensity of ThT fluorescence is proportional to the amount of fibril-bound dye, we managed to reproduce the fluorescence dependencies on the CR concentration with meaningful sets of the binding parameters, as illustrated in figures 4(A) and (B) (see also supplementary figure 2). Although we have demonstrated the principal possibility of ThT displacement from the fibril binding sites, there are some reasons to be skeptical about the ThT–CR competition model. First, to fit the experimental data obtained for apoA-I(1–83) we used rather high CR association constants ($K_a^{CR} \sim 85$). Second, previous studies, despite being performed with other types of proteins, state that ThT and CR could have different

Figure 7. Fluorescence intensity of CR at 610 nm plotted versus the dye concentration: (A) an N-terminal fragment of apoA-I, (B) Ins, (C) Lz. The protein concentrations were: 0.5 μM (apoA-I(1–83)), 5 μM (Ins), 10 μM (Lz).

binding sites within amyloid fibrils [36]. Third, it has been shown that CR analogue K114 is unable to compete with ThT and uncharged ThT analogue thioflavin S is unable to compete with CR [10, 27]. Finally, several polyphenolic compounds have been reported to interact with ThT but not with CR in the presence of amyloid fibrils [37].

A second possible reason for the CR-induced quenching of ThT fluorescence is direct ThT–CR complexation in the cavities of amyloid β-sheets. Such a complexation can be governed by the hydrophobic interactions between planar groups of the dye molecules, and by the ionic nature of the positively charged ThT and negatively charged CR. At least one study describes the formation of ThT–CR clusters on the surface of Ab(1–42) amyloid fibrils, although the employed quartz-crystal microbalance method is not sensitive enough to detect any complexation at dye concentrations below the critical micelle concentration (CMC) [35].

A third reason for the observed suppression of ThT fluorescence by CR involves the FRET between fibril-bound ThT as a donor and CR as an acceptor (figure 5). Indeed, as seen in figure 3, the intensity decrease at the ThT emission maximum and a corresponding intensity increase at the CR emission maximum could be considered to be FRET that mimics the above described displacement and complexation models of ThT fluorescence

quenching. Moreover, the possibility of such FRET is supported by the following considerations. Due to the strong overlap between ThT emission and CR absorption spectra, the energy can be transferred between these dyes by a distance-dependent Förster mechanism with the critical distance of energy transfer (R_o) as large as 4 nm (figure 5). According to the 'channel' model of ThT- and CR-fibril binding, these dyes reside along surface side-chain grooves running parallel to the long fibril axis [21, 38, 39]. Taking the propagation of an extended polypoptide chain as 0.35 nm per residue and a thickness of amyloid core as 1 nm, in recently proposed structures of amyloid protofilaments of the studied proteins the maximum proximity between such grooves (which is approximately equal to the length of protofilament core) is 5.7 nm, 3.4 nm and 4.3 nm for apoA-I [32], Ins [30] and Lz [31], respectively. Therefore, it seemed reasonable to assume that, notwithstanding the actual positions of bound donors and acceptors, at least part of the ThT excitation energy is transferred by means of FRET. Based on this assumption, we simulated the ThT–CR FRET using the stretched exponential model describing energy transfer in the spatially confined molecular systems [40]:

$$Q_r = \int_0^\infty \exp\left(-\lambda - C_A V_d \Gamma(1 - d/6)\lambda^{\frac{d}{6}}\right)d\lambda \qquad (4)$$
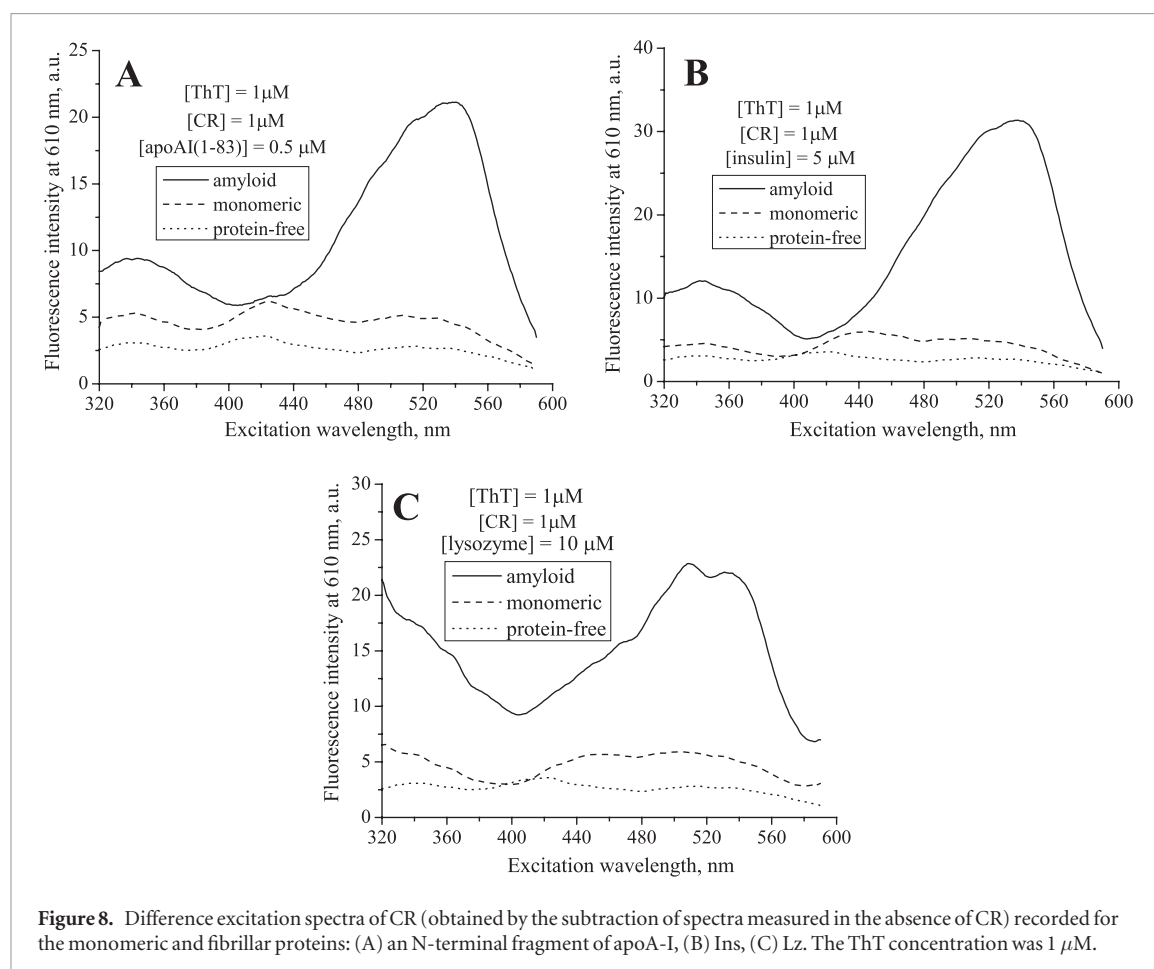
Figure 8. Difference excitation spectra of CR (obtained by the subtraction of spectra measured in the absence of CR) recorded for the monomeric and fibrillar proteins: (A) an N-terminal fragment of apoA-I, (B) Ins, (C) Lz. The ThT concentration was 1 μM.

where $\lambda = t/\tau_D$, τ_D is the donor fluorescence lifetime in the absence of an acceptor; $V_d = \pi \frac{d}{2} R_o^d / \Gamma \left(\frac{d}{2} + 1 \right)$ is the volume of the d-dimensional sphere of radius R_o, d is the dimensionality of the fluorophore distribution (fractal-like dimension), which depends on the scaling between the mass and size of the polypeptide chain, being a measure of protein compactness, $C_A = B_{CR}/PV_{PF}$, and V_{PF} is the volume of the protein molecule in a fibrillar state. Since the parameters V_{PF} and d are presently known only for fibrillar Lz [41], we analyzed the ThT fluorescence profiles obtained for this protein (figure 4(C)), just to illustrate that ThT–CR FRET can contribute to the observed effects. First, we made an attempt to approximate the experimental data by equation (4), assuming that all the fibrillar volume is accessible to the acceptor (coefficient of accessibility $\alpha = 1$) and taking the R_o value valid for the isotropic and dynamic averaging conditions, when donors and acceptors are rapidly tumbling and their transition dipoles can adopt all orientations in a time that is short compared with the transfer time ($\kappa^2 = 0.67$). However, in this case there was a marked disagreement between theory and experiment (figure 4(C)). Therefore, it was logical to suppose that the rotational mobility of the donors and acceptors is substantially restricted in a fibrillar environment and the orientation factor κ^2 was allowed to vary within the widest possible limits corresponding to perpendicular ($\kappa^2 = 0$) and parallel orientation of the donor and acceptor dipoles

($\kappa^2 = 4$) [29]. It appeared that a sharp initial drop in ThT fluorescence, observed at CR concentrations less than 0.1 μM, can be adequately described by the employed model with the parameter set, $\{\kappa^2 = 4, \alpha = 0.3, d = 3\}$, on the assumption that CR-fibril binding is virtually complete. Although we failed to reproduce the whole experimental curve, the performed simulation clearly demonstrates that the FRET between ThT and CR can be implicated in the CR-induced ThT fluorescence quenching. Overall, regardless of the exact mechanism of the ThT fluorescence decrease in the presence of CR, it is evident that this phenomenon can be considered as a sign of amyloid formation.

3.2. Amyloid-specific changes in the excitation and emission spectra of CR

Along with the decrease in ThT fluorescence, the association of CR with amyloid fibrils provokes the appearance of a pronounced peak at ~530–540 nm in the CR excitation spectra (figure 6). This excitation peak reflects a well-known CR property that it undergoes a shift in the absorption maximum from 498 nm to 540 nm upon binding to β-sheet cavities of amyloid protofilaments [15]. The CR spectral shift is accompanied by a drastic absorbance increase at 540 nm and enhancement of the dye fluorescence at 610 nm, presumably because of restricted fluorophore mobility in the fibril environment. As illustrated in figure 7, the fluorescence intensity increase at 610 nm is

much more pronounced for fibrillar protein. Moreover, such CR spectral changes can be considered to be one of the strongest criteria for the presence of true amyloid fibrils. Indeed, we failed to detect the appearance of the amyloid-specific CR spectral changes in ThT mixtures with monomeric proteins, although there was some increase in the overall intensity of the excitation spectra (figure 8).

In principle, it is possible to get the following parameters of CR binding: association constant, binding stoichiometry and the change in CR quantum yield. The problem is that, due to the number of parameters to be extracted one needs to have a 2D set of data with the varying of both the protein and the dye concentrations. Once obtained the parameters will be useful for localization of CR binding sites within the amyloid core and, hence, for the elucidation of the fibril structure. On the other hand, such binding parameters can be used as a basis for assessing the amount of amyloid in the sample.

Taken together, our findings highlight the following indications of amyloid formation while simultaneously probing the examined system with ThT and CR:

(1) a common drastic increase in ThT fluorescence intensity;

(2) a sharp decrease (more than 50%) of ThT fluorescence upon addition of CR in sub-micromolar concentrations;

(3) an appearance of a maximum at 535–540 nm in CR excitation spectra measured at emission wavelength 610 nm;

(4) an increase in CR fluorescence intensity at 610 nm.

It is important to note that the optimal conditions for the implementation of the above assay include: (i) ThT concentration of 1–4 μM, below its CMC; (ii) the CR-to-ThT molar ratio falling in the range 0.01–1; (iii) a protein concentration of less than 10 μM is sufficient to produce a desirable spectral response.

4. Conclusions

To summarize, the present study has been undertaken to design a fluorescence-based ThT–CR test for amyloid detection. The proposed combined ThT–CR assay has been successfully verified by analyzing the fibrillar aggregates formed by three different amyloidogenic proteins: N-terminal fragment of apoA-I, Ins and Lz. The results obtained strongly suggest that the proposed approach can be applied to a wide variety of amyloid proteins that are predetermined by their ability to induce similar changes in the spectral behavior of ThT and CR [4]. The combined ThT–CR method has several advantages over the classical single-dye approaches. First, this method requires one sample and a common spectrofluorimeter. Second, it is rapid and simple and can be performed together with

kinetic ThT fluorescence measurements. Third, the designed assay provides a synergistic increase of ThT and CR specificity for amyloid aggregates, allowing the minimization of false positive or negative results. Finally, this approach allows the elimination of the drawbacks inherent to ThT and CR tests when used separately, and gives us a convenient and handy tool for accurately determining the extent of amyloid formation at a given time point.

References

[1]   Stefani M 2004 Protein misfolding and aggregation: new examples in medicine and biology of the dark side of the protein world *Biochim. Biophys. Acta* **1739** 5–25

[2]   Idicula-Thomas S and Balaji P V 2007 Protein aggregation: a perspective from amyloid and inclusion body formation *Curr. Sci.* **92** 758–67

[3]   Makin O S and Serpell L C 2005 Structures for amyloid fibrils *FEBS J.* **272** 5950–61

[4]   Groenning M 2010 Binding mode of Thioflavin T and other molecular probes in the context of amyloid fibrils—current status *J. Chem. Biol.* **3** 1–18

[5]   Naiki H, Higuchi K, Hosokawa M and Takeda T 1989 Fluorometric determination of amyloid fibrils *in vitro* using the fluorescent dye, Thioflavin T *Anal. Biochem.* **177** 244–9

[6]   LeVine H 1993 Thioflavin T interaction with synthetic Alzheimer's disease β-amyloid peptides: detection of amyloid aggregation in solution *Protein Sci.* **2** 404–10

[7]   Sulatskaya A I, Maskevich A A, Kuznetsova I M, Uversky V N and Turoverov K K 2010 Fluorescence quantum yield of Thioflavin T in rigid isotropic solution and incorporated into the amyloid fibrils *PLoS One* **5** e15385

[8]   Stsiapura V I, Maskevich A A and Kuznetsova I M 2007 Computational study of Thioflavin T torsional relaxation in the excited state *J. Phys. Chem.* A **111** 4829–35

[9]   Hawe A, Sutter M and Jiskoot W 2008 Extrinsic fluorescent dyes as tools for protein characterization *Pharm. Res.* **25** 1487–99

[10] De Ferrari G V, Mallender W D, Inestrosa N C and Rosenberry T L 2001 Thioflavin T is a fluorescent probe of the acetylcholinesterase peripheral site that reveals conformational interactions between the peripheral and acylation sites *J. Biol. Chem.* **276** 23282–7

[11] Groenning M, Olsen L, van de Weert M, Flink J M, Frokjaer S and Jørgensen F S 2007 Study on the binding of Thioflavin T to beta-sheet-rich and non-beta-sheet cavities *J. Struct. Biol.* **158** 358–69

[12] Carrotta R, Bauer R, Waninge R and Rischel C 2001 Conformational characterization of oligomeric intermediates and aggregates in β-lactoglobulin heat aggregation *Protein Sci.* **10** 1312–8

[13] Kumar S, Singh A K, Krishnamoorthy G and Swaminathan R 2008 Thioflavin T displays enhanced fluorescence selectively inside anionic micelles and mammalian cells *J. Fluoresc.* **18** 1199–205

[14] Ilanchelian M and Ramaraj R 2004 Emission of Thioflavin T and its control in the presence of DNA *J. Photochem. Photobiol.* A **162** 129–37

[15] Klunk W E 1989 Quantitative evaluation of Congo Red binding to amyloid-like proteins with a beta-pleated sheet conformation *J. Histochem. Cytochem.* **37** 1273–81

[16] Schutz A K, Soragni A, Hornemann S, Aguzzi A, Ernst M, Bockmann A and Meier B 2011 The amyloid–Congo Red interface at atomic resolution *Angew. Chem. Int. Ed.* **50** 5956–60

[17] Turnell W G and Finch J T 1992 Binding of the dye Congo Red to the amyloid protein pig insulin reveals a novel homology amongst amyloid-forming peptide sequences *J. Mol. Biol.* **227** 1205–23

[18] Carter D B and Chou K C 1998 A model for structure-dependent binding of Congo Red to Alzheimer β-amyloid fibrils *Neurobiol. Aging* **19** 37–40

[19] Romhanyi G 1971 Selective differentiation between amyloid and connective tissue structures based on the collagen specific topo-optical staining reaction with Congo Red *Virchows Arch. A, Pathol. Anat. Histopathol.* **354** 209–22

[20] Cooper J H 1974 Selective amyloid staining as a function of amyloid composition and structure. Histochemical analysis of the alkaline Congo Red, standardized toluidine blue, and iodine methods *Lab. Invest.* **31** 232–8

[21] Krebs M R H, Bromley E H C and Donald A M 2005 The binding of Thioflavin-T to amyloid fibrils: localisation and implications *J. Struct. Biol.* **149** 30–7

[22] Frid P, Anisimov S V and Popovic N 2007 Congo Red and protein aggregation in neurodegenerative diseases *Brain. Res. Rev.* **53** 135–60

[23] Khurana R, Uversky V N, Nielsen L and Fink A 2001 Is Congo red an amyloid-specific dye? *J. Biol. Chem.* **276** 22715–21

[24] Nilsson M R 2004 Techniques to study amyloid fibril formation *in vitro Methods* **34** 151–60

[25] Adachi E, Nakajima H, Mizuguchi C, Dhanasekaran P, Kawashima H, Nagao K, Akaji K, Lund-Katz S, Phillips M C and Saito H 2013 Dual role of an N-terminal amyloidogenic mutation in apolipoprotein A-I: destabilization of helix bundle and enhancement of fibril formation *Biochem. J. Biol. Chem.* **288** 2848–56

[26] Jansen R, Grudzielanek S, Dzwolak W and Winter R 2004 High pressure promotes circularly shaped insulin amyloid *J. Mol. Biol.* **338** 203–6

[27] Frare E, Polverino De Laureto P, Zurdo J, Dobson C M and Fontana A 2004 A highly amyloidogenic region of hen lysozyme *J. Mol. Biol.* **340** 1153–65

[28] Bulychev A A, Verchoturov V N and Gulaev B A 1988 *Current Methods of Biophysical Studies* (Moscow: Vyschaya Shkola)

[29] Lakowicz J R 2006 *Principles of Fluorescent Spectroscopy* (New York: Springer)

[30] Kurouski D, Washington J, Ozbil M, Prabhakar R, Shekhtman A and Lednev I K 2012 Disulfide bridges remain intact while native insulin converts into amyloid fibrils *PLoS One* **7** e36989

[31] Tokunaga Y, Sakakibara Y, Kamada Y, Watanabe K and Sugimoto Y 2013 Analysis of core region from egg white lysozyme forming amyloid fibrils *Int. J. Biol. Sci.* **9** 219–27

[32] Girych M, Gorbenko G, Trusova V, Adachi E, Mizuguchi C, Nagao K, Kawashima H, Akaji K, Phillips M and Saito H 2014 Interaction of Thioflavin T with amyloid fibrils of apolipoprotein A-I N-terminal fragment: resonance energy transfer study *J. Struct. Biol.* **185** 116–24

[33] Lendel C, Bertoncini C W, Cremades N, Waudby C A, Vendruscolo M, Dobson C M, Schenk D, Christodoulou J and Toth G 2009 On the mechanism of nonspecific inhibitors of protein aggregation: dissecting the interactions of alpha-synuclein with Congo Red and lacmoid *Biochemistry* **48** 8322–34

[34] LeVine H 2005 Mechanism of Aβ(1–40) Fibril-Induced Fluorescence of (trans,trans)-1-Bromo-2,5-bis (4-hydroxystyryl)benzene (K114) *Biochemistry* **44** 15937–43

[35] Buell A K, Dobson C M, Knowles T P J and Welland M E 2010 Interactions between amyloidophilic dyes and their relevance to studies of amyloid inhibitors *Biophys. J.* **99** 3492–7

[36] Zhuang Z P, Kung M P, Hou C, Skovronsky D M, Gur T L, Plössl K, Trojanowski J Q, Lee V M and Kung H F 2001 Radioiodinated styrylbenzenes and Thioflavins as probes for amyloid aggregates *J. Med. Chem.* **44** 1905–14

[37] Hudson S A, Ecroyd H, Kee T W and Carver J A 2009 The Thioflavin T fluorescence assay for amyloid fibril detection can be biased by the presence of exogenous compounds *FEBS J.* **276** 5960–72

[38] Biancalana M, Makabe K, Koide A and Koide S 2008 Aromatic cross-strand ladders control the structure and stability of beta-rich peptide self-assembly mimics *J. Mol. Biol.* **383** 205–13

[39] Wu C, Scott J and Shea J E 2012 Binding of Congo Red to amyloid protofibrils of the Alzheimer Aβ9–40 peptide probed by molecular dynamics simulations *Biophys J.* **103** 550–7

[40] Drake J M, Klafter J and Levitz P 1991 Chemical and biological microstructures as probed by dynamic processes *Science* **251** 1574–9

[41] Gorbenko G, Trusova V, Kirilova E, Kirilov G, Kalnina I, Vasilev A, Kaloyanova S and Deligeorgiev T 2010 New fluorescent probes for detection and characterization of amyloid fibrils *Chem. Phys. Lett.* **495** 275–9